Fourier Feature Refiner Network With Soft Thresholding for Machinery Fault Diagnosis Under Highly Noisy Conditions

Huan Wang, *Graduate Student Member, IEEE*, Wenjun Luo, Zhiliang Liu, *Member, IEEE*, Junhao Zhang, *Graduate Student Member, IEEE*, and Mingjian Zuo, *Senior Member, IEEE*

***Abstract*—Machinery fault diagnosis plays an important role in machine prognostic and health management (PHM). Leveraging the abundant data obtained from the Industrial Internet of Things (IIoT), the health states of machines can be effectively recognized, thereby ensuring the safety of the mechanical system. However, the lack of noise robustness and insufficient frequency domain perception make traditional methods to extract weak fault-related signals difficult under highly noisy conditions in practical industrial scenarios. Therefore, a method with abundant frequency domain learning ability is urgently needed. To this end, this article proposes a PHM framework, a soft thresholding Fourier feature refiner network (Soft-FFRNet), for highly noisy bearing vibration signal diagnosis. Specifically, this framework includes a Fourier feature refiner which selectively extracts and refines the feature in the frequency domain from the perspectives of amplitude and phase. It achieves the extension from the time domain to the frequency domain. In addition, the proposed framework utilizes several residual blocks with soft thresholding to effectively improve the noise robustness. Their thresholds can adaptively change during the training process. The high-speed aeronautical (HSA) bearing and the motor bearing data sets with different noise levels are used to evaluate this framework. The results show that the proposed framework can effectively diagnose the faults under highly noisy conditions.**

***Index Terms*—Deep learning, Fourier transform, machinery fault diagnosis, noise robustness, prognostic and health management (PHM).**

Manuscript received 5 December 2023; revised 16 January 2024; accepted 22 January 2024. Date of publication 7 February 2024; date of current version 26 June 2024. This work was supported in part by the Sichuan Provincial Key Research and Development Program under Grant 2023YFG0351, and in part by the National Natural Science Foundation of China under Grant 61833002. *(Huan Wang and Wenjun Luo contributed equally to this work.) (Corresponding author: Zhiliang Liu.)*

Huan Wang is with the School of Mechanical and Electrical Engineering, University of Electronic Science and Technology of China, Chengdu 611731, China, and also with the Department of Industrial Engineering, Tsinghua University, Beijing 100084, China.

Wenjun Luo and Junhao Zhang are with the Glasgow College, University of Electronic Science and Technology of China, Chengdu 611731, China.

Zhiliang Liu is with the School of Mechanical and Electrical Engineering, University of Electronic Science and Technology of China, Chengdu 611731, China (e-mail: Zhiliang_Liu@uestc.edu.cn).

Mingjian Zuo is with Qingdao International Academician Park Research Institute, Qingdao 266041, China, also with the School of Mechanical and Electrical Engineering, University of Electronic Science and Technology of China, Chengdu 611731, China, and also with the Department of Mechanical Engineering, University of Alberta, Edmonton, AB T6G 1H9, Canada (e-mail: ming.zuo@ualberta.ca).

Digital Object Identifier 10.1109/JIOT.2024.3363216

I. Introduction

DUE TO the rapid developments in science and technology, and the expansion of modern industries, machinery equipment is now utilized daily across various applications [1]. However, these machines often operate under challenging conditions, such as high humidity and excessive loads. Consequently, some faults may occur, resulting in substantial maintenance costs, significant financial losses, potentially reduced productivity, and even posing a potential risk to human lives. Thus, it is vital to monitor the health states of critical components of mechanical systems to ensure their reliability and safety [2]. Thanks to the emergence and rapid development of Industrial Internet of Things (IIoT) technologies, vast amounts of data on devices are available for the development of prognostic and health management (PHM) frameworks [3], [4], [5]. The diagnostic results can contribute to decision-making processes for predictive maintenance, replacement, and asset management [6]. In addition, the application of IIoT enables the real-time monitoring of machine health states through IIoT sensors, facilitating prompt alerts for potential faults [7].

Traditionally, before the emergence of IIoT, engineers relied on their expert knowledge to diagnose faults in machines based on monitoring data [2], [8]. However, with the rapid development of modern industries, the demand for automatic diagnosis methods has grown [9]. With the help of machine learning theories, the relationship between collected data and the health states of the machine is bridged [2]. The procedure of machine learning fault diagnosis methods mainly contains artificial feature extraction, and health state recognition [2], [10]. The step of artificial feature extraction focuses on extracting fault-related features in the collected data from different perspectives. In the step of health state recognition, to build links between these features and the health state of machines, some machine learning-based diagnosis models are employed, such as expert systems [11], artificial neural networks (ANNs) [12], [13], and support vector machine (SVM) [14]. Unal et al. [15] proposed methods to extract features using envelope analysis accompanied by the Hilbert Transform and fast Fourier transform (FFT). Zheng et al. [16] proposed a rolling bearing fault diagnosis method based on the composite multiscale fuzzy entropy (CMFE) and ensemble SVMs (ESVMs) to detect the incipient failure of rolling bearing. However, the methods implemented in the process

of artificial feature extraction will significantly affect the diagnostic accuracy of these recognition methods. In other words, it requires corresponding expert knowledge for each specific fault diagnosis task, which is unrealistic because of its vast labor cost. Moreover, the architectures of these recognition methods are shallow, which means it is hard for them to learn sufficient features.

Currently, in the field of machinery fault diagnosis, deep learning-based methods have gained significant attention for their capability to leverage deep architecture models to automatically extract rich abstract features from the big data set without relying on expert knowledge and further diagnose the health states of the machines [2]. Meanwhile, with the development of IIoT technologies, the volume of data has dramatically increased, which can provide sufficient information for deep models. Therefore, various deep learning-based diagnosis algorithms have been extensively studied and applied to machinery fault diagnosis [17], [18], [19]. Li et al. [20] proposed a novel deep sparse autoencoder with lossless and nonnegative constraints for intelligent fault diagnosis of rotating machinery, which performs well on the CWRU bearing data set. Based on the self-attention mechanism and graph neural network (GNN), Zhang et al. [21] proposed a multisensor multihead graph attention network to fuse multisource features for large rotating machinery fault diagnosis, which can dynamically fuse and mine the high-level fault characteristics. Notably, convolutional neural networks (CNNs) [22], [23], [24], [25] outperform other methods in various machinery fault diagnosis tasks. Zhao et al. [26] proposed a normalized CNN, which utilizes batch normalization (BN) to eliminate feature distribution differences of different fault severities and orientations considering data imbalance and variable working conditions. Xu et al. [27] proposed a multiattention-based feature aggregation convolutional network (MFACN). It designs an attention-based multiscale module (AMM) and a multiscale feature aggregation module (MFAM) to facilitate comprehensive learning across multiple levels. Wang et al. [28] proposed a CNN using the generalized neighborhood preserving embedding (GNPE) method to enhance the feature extraction and generalization capabilities.

Although these deep model researches can reach a satisfactory performance, they still have the following problems.

1) The collected vibration signals of bearings are often mixed with strong environmental noise. The fault-related components can be easily overwhelmed by noise. However, these methods lack noise robustness, rendering them unable to extract valuable information from strong and complex noise.
2) Each IIoT sensor operates under different working conditions. The variability in noise between different IIoT sensors implies that conventional filters with static parameters are insufficient for noise elimination. Thus, it is necessary to endow the network with an adaptive nonlinear threshold.
3) Traditional time domain-based deep models have deficiencies in frequency domain perception. They cannot effectively comprehend and utilize the frequency characteristics of signals. This inadequacy in frequency domain perception can result in overlooking critical fault-related features inherent in the frequency domain, thereby hindering the extraction of subtle fault-related features from strong environmental noise.

Compared with time domain analysis, frequency domain analysis has several advantages.

1) Frequency domain analysis allows for the separation of signal components at different frequencies. It is possible to distinguish between the desired fault-related components and unwanted noise components.
2) Frequency domain analysis can enhance fault-related feature extraction. Fault-related features in the frequency domain are more pronounced and distinguishable than in the time domain.
3) Frequency domain analysis can help with noise reduction. By identifying fault-related frequencies, harmonics, or amplitude modulations in the frequency domain, it can reduce or eliminate noise while preserving fault-related information.

Motivated by these advantages of frequency domain analysis, many researchers are trying to integrate it into deep learning methods. Lin et al. [29] proposed a stacked autoencoder network (SAE). In their method, the original time domain signals are transformed into frequency domain signals by FFT before the training process. Huang et al. [30] also utilized a fractional Fourier transform to preprocess the time domain signal before diagnosis. They merely used frequency domain analysis as a preprocessing step, and then utilized a classification model for fault diagnosis, failing to learn the frequency domain features adaptively.

To address the limitations mentioned above, this article explores to analyze features adaptively from the frequency domain. This article introduced a soft thresholding Fourier feature refiner network (Soft-FFRNet) to improve the noise robustness and frequency domain perception. Specifically, to effectively distinguish the fault-related features, the proposed fault diagnosis framework integrates a novel Fourier feature refiner. By introducing the FFT, we have endowed the model with frequency domain learning ability. It can discover fault-related features from the frequency domain, which is inaccessible from the time domain. The feature refiner decomposes the complex features obtained by FFT into amplitude components and phase components. Thus, it provides more perspectives to refine the extracted features. Meanwhile, this article proposes a soft thresholding-based residual block, which utilizes residual connections to enable fast gradient propagation. Additionally, the rectified linear unit (ReLU) function is replaced by soft thresholding to provide better nonlinear transformation and adaptive noise reduction. By combining the Fourier feature refiner with soft thresholding-based residual blocks, the proposed Soft-FFRNet can effectively diagnose the faults under strong environmental noise.

To demonstrate the effectiveness of our model, this article conducts an experiment on the high-speed aeronautical (HSA) bearing and the motor bearing data sets. The results show that our model can significantly improve diagnostic accuracy in highly noisy conditions.

The contributions of this article are summarized as follows.

1) This article proposes a Fourier feature refiner, which endows the model with frequency domain learning ability. It extracts and refines the features in the frequency domain from the perspectives of amplitude spectral and phase spectral, and enhances the fault-related components accordingly.
2) This article proposes soft thresholding-based residual blocks, which utilize adaptive thresholds to tackle various noises under different working conditions, thereby preserving the main fault-related features while reducing noise.
3) This article proposes a fault diagnosis framework (Soft-FFRNet) for highly noisy bearing vibration signal diagnosis, which employs a Fourier feature refiner and uses soft thresholding-based residual blocks as the backbone to accurately diagnose bearing faults in a strong noise environment.
4) The proposed Soft-FFRNet is thoroughly evaluated on two real-life vibration signal data sets under different noise levels, and the experiments show that it has excellent noise robustness diagnostic capability.

The remainder of this article is organized as follows: Section II describes the proposed Soft-FFRNet in detail. Section III shows the details of the experiment, ablation study, and comparison with earlier works. Section IV discusses the effectiveness of the proposed methods. Section V summarizes this article.

II. Methodology

A. Overview of Soft-FFRNet

This article proposes a novel fault diagnosis framework, Soft-FFRNet, based on an innovative Fourier feature refiner with soft thresholding-based residual blocks to effectively diagnose machinery faults under highly noisy conditions. The overall framework is shown in Fig. 1.

To better discover fault-related information from highly noisy signals, the proposed framework adopts an innovative Fourier feature refiner after the first convolutional layer, which enables the framework to learn in the frequency domain. The feature refiner decomposes and views the feature from amplitude spectral and phase spectral perspectives. For these two components, two learnable feature refiners are employed to adaptively refine them, respectively. It enables fault-related features to be effectively extracted and refined, while noise-related features can be reduced or eliminated. Moreover, residual blocks with soft thresholding are employed to handle noisy signals under various working conditions. They provide an adaptive nonlinear transformation to mitigate different kinds of noise adaptively. Five soft thresholding-based residual blocks are stacked in a way that gradually increases the number of channels so that valuable information can be learned. Finally, the learned high-level features are fed into a fully connected layer for classification.

B. Fourier Feature Refiner

Traditional machinery fault diagnosis algorithms rely on time-domain feature extraction. However, under highly noisy conditions, weak fault-related features in the time domain are prone to be masked by environmental noise. In contrast, fault-related features are more prominent and distinguishable in the frequency domain. Therefore, it is necessary to empower the model to learn fault-related features from the frequency domain. The proposed Fourier feature refiner is a module capable of achieving this purpose.

The overall structure of the Fourier feature refiner can be found in Fig. 1. Given an input feature ϖ of shape ($\mathbb{R}^{C\times L}$) which is obtained from decomposing the input signal by a 1-D convolutional layer. First, this input feature is transformed into frequency domain channel by channel using Fourier transform. The 1-D discrete Fourier transform (DFT) of the length-L time domain sequence $\varpi_i[l]$ is defined as follows:

$$\varpi_i^{\mathrm{DFT}}[k]=\sum_{l=0}^{L-1}\varpi_i[l]e^{-j2\pi kl/L},\ 0\leqslant k\leqslant L-1 \tag{1}$$

where $\varpi_i[l]$ denotes the ith channel of input feature ϖ; $\varpi_i^{\mathrm{DFT}}[k]$ denotes the kth DFT coefficient of the ith channel feature; $i=1,2,\ldots,C$; $j=\sqrt{-1}$ represents the imaginary number.

After implementing DFT to each channel, the result ϖ^{DFT} remains the shape of $\mathbb{R}^{C\times L}$, however, the elements are complex numbers. Then, these elements are decomposed into amplitude components and phase components. Since the elements of the input feature ϖ are real numbers, the amplitude component and phase component can be calculated by using the following properties:

$$\varpi_i^{\mathrm{DFT}}[k]=\sum_{l=0}^{L-1}\varpi_{i,\mathrm{re}}[l]\cos\left(\frac{2\pi kl}{L}\right)-j\sum_{l=0}^{L-1}\varpi_{i,\mathrm{re}}[l]\sin\left(\frac{2\pi kl}{L}\right) \tag{2}$$

$$\varpi_{i,\mathrm{re}}^{\mathrm{DFT}}[k]=\sum_{l=0}^{L-1}\varpi_{i,\mathrm{re}}[l]\cos\left(\frac{2\pi kl}{L}\right) \tag{3}$$

$$\varpi_{i,\mathrm{im}}^{\mathrm{DFT}}[k]=-\sum_{l=0}^{L-1}\varpi_{i,\mathrm{re}}[l]\sin\left(\frac{2\pi kl}{L}\right) \tag{4}$$

$$\left|\varpi_i^{\mathrm{DFT}}[k]\right|=\sqrt{\varpi_{i,\mathrm{re}}^{\mathrm{DFT}}[k]^2+\varpi_{i,\mathrm{im}}^{\mathrm{DFT}}[k]^2} \tag{5}$$

$$\angle\varpi_i^{\mathrm{DFT}}[k]=\arctan\left(\frac{\varpi_{i,\mathrm{im}}^{\mathrm{DFT}}[k]}{\varpi_{i,\mathrm{re}}^{\mathrm{DFT}}[k]}\right) \tag{6}$$

where $\varpi_{i,\mathrm{re}}^{\mathrm{DFT}}[k]$ and $\varpi_{i,\mathrm{im}}^{\mathrm{DFT}}[k]$ represent the real and imaginary part of $\varpi_i^{\mathrm{DFT}}[k]$, respectively; $\left|\varpi_i^{\mathrm{DFT}}[k]\right|$ and $\angle\varpi_i^{\mathrm{DFT}}[k]$ represent the amplitude component and phase component of $\varpi_i^{\mathrm{DFT}}[k]$. Therefore, ϖ^{DFT} can be represented by $\left|\varpi_i^{\mathrm{DFT}}[k]\right|e^{j\angle\varpi_i^{\mathrm{DFT}}[k]}$. For convenience, later in this article, we use A to represent $\left|\varpi_i^{\mathrm{DFT}}[k]\right|$ and ϕ to represent $\angle\varpi_i^{\mathrm{DFT}}[k]$.

Next, the amplitude component A and phase component ϕ are multiplied with their corresponding learnable feature refiner to provide a frequency domain-based feature extraction and refinement

$$\bar{A}=\alpha\otimes A \tag{7}$$

$$\bar{\phi}=\beta\otimes\phi. \tag{8}$$

Here, $\otimes$ denotes element-wise multiplication. $\bar{A}$ and $\bar{\phi}$ indicate their values after refinement. α and β indicate the weight

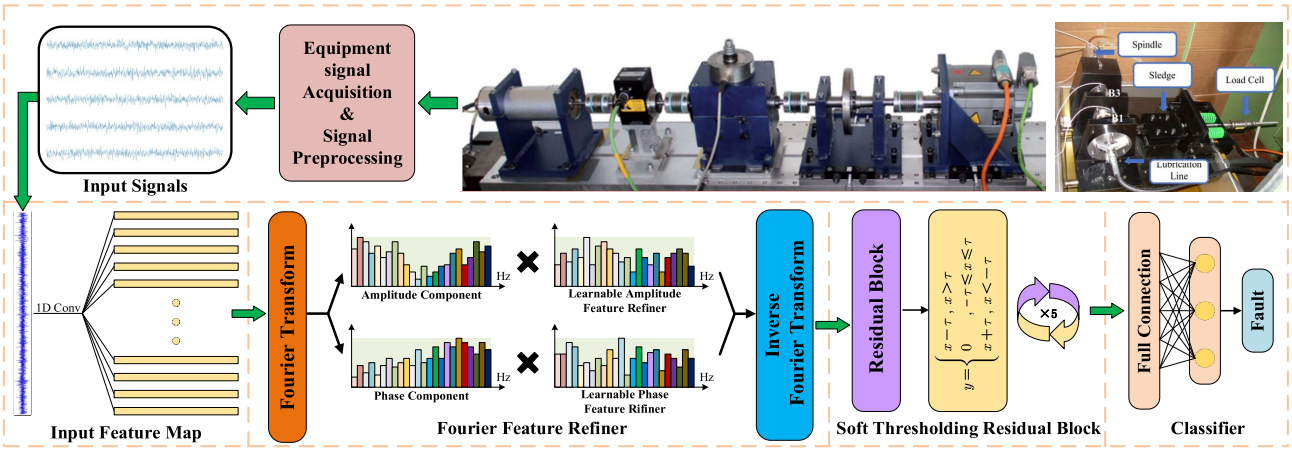

Fig. 1. Detailed network architecture of the proposed Soft-FFRNet.

of each frequency component. The magnitude of their value indicated the importance of the corresponding frequency. Since each fault category typically has its corresponding fault characteristic frequency, by enhancing the fault-related frequency components and attenuating other irrelevant frequency components, the fault-related features will be more prominent and thus improve the fault diagnostic accuracy.

Finally, the refined components are reconstructed as follows:

$$\varpi^{\mathrm{REC}} = |\bar{A}|e^{j\bar{\phi}} \tag{9}$$

and the refined feature is transformed back to the time domain by the inverse discrete Fourier transformation (IDFT) channel by channel

$$\varpi_i'[l] = \frac{1}{L}\sum_{k=0}^{L-1} \varpi_i^{\mathrm{REC}}[k]e^{j2\pi kl/L}, 0 \leqslant l \leqslant L-1. \tag{10}$$

C. Soft Thresholding-Based Residual Block

The soft thresholding-based residual block uses a soft thresholding mechanism [31] to adaptively reduce different kinds of noise under various working conditions. Suppose the input feature ψ to be expressed as follows:

$$\psi = \chi + \epsilon \cdot z \tag{11}$$

where χ represents fault-related features; z denotes-noised related features and ϵ denotes noise level. The goal is to propose a transformation that can preserve χ while reducing $\epsilon \cdot z$ as much as possible, i.e., a transformation $f(\psi)$ that satisfies

$$\min_{f(\psi)} \|f(\psi) - \chi\|_F \tag{12}$$

where $\|\cdot\|_F$ means Frobenius-norm. The equation above describes the intention of finding a transformation $f(\psi)$ that removes noise-related features while retaining valuable fault-related features. However, in real-world applications, determining $f(\psi)$ and χ poses a significant challenge.

Generally, Gaussian white noise is widely used to simulate noise disturbances in mechanical systems since it possesses statistical properties observed in real-world disturbances.

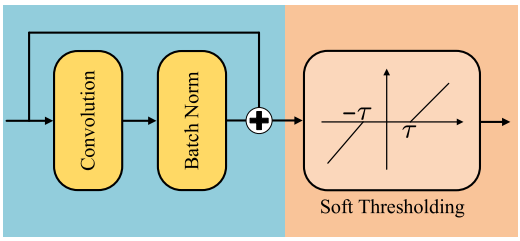

Fig. 2. Structure of soft thresholding-based residual block.

Gaussian white noise distributes its energy uniformly across all frequencies. Therefore, most noise-related features are represented by relatively small components, whereas fault-related features are manifested as larger components at several specific positions. Consequently, we can eliminate the noise while preserving the main signal by setting a threshold. Based on this, we propose a soft thresholding-based residual block.

The structure of the proposed method is shown in Fig. 2. It consists of a residual block and a dynamic nonlinear transformation. The soft thresholding function can be expressed as follows:

$$y = \begin{cases} x - \tau, & x > \tau \\ 0, & -\tau \leqslant x \leqslant \tau \\ x + \tau, & x < -\tau \end{cases} \tag{13}$$

where τ represents the dynamic threshold. This function is intuitively shown in the right part of Fig. 2. It can also be expressed equivalently as follows:

$$y = \mathrm{sign}(x)\max(|x| - \tau, 0). \tag{14}$$

However, it is challenging to manually find a suitable threshold τ under various noise conditions. Hence, we utilize the information learned by deep learning to automatically determine one. Assuming the shape of the feature transmitted from the previous network is $\mathbb{R}^{C\times L}$. Its calculated procedure is shown below.

First, calculate the average absolute value of the cth channel

$$\vartheta_c = \sum_{i=0}^{L-1} |x_{c,i}|. \tag{15}$$

Then, a scaling factor ϱ is extracted from ϑ by using a two-layer fully connected network (FCN)

$$\varrho = \text{Sigmoid}(\text{FCN}(\vartheta)). \tag{16}$$

Finally, by multiplying these two parameters channel by channel, the threshold τ_c for each channel is calculated

$$\tau_c = \varrho_c \cdot \vartheta_c. \tag{17}$$

Since the factor ϱ is constrained to be between $(0, 1)$ by the sigmoid function, it can be ensured that the threshold τ_c will never exceed the maximum value within its channel, thereby guaranteeing that the output of the soft-thresholding function will not all become zero.

Compared with the work proposed in [32], the block proposed in this article brings the shortcut connection of the residual block before the soft thresholding to prevent noise leakage along the shortcut of the residual connection. Moreover, since the property of the ReLU function is similar to soft thresholding, which means it may overwhelm the effect of soft thresholding, the proposed block removes the ReLU function in the residual block. Also, the number of convolutional layers between the residual connections is reduced to one layer to prevent overfitting. In short, the proposed soft thresholding-based block is simpler but more effective.

D. Implementation Details

The proposed Soft-FFRNet is specially designed for PHM under highly noisy conditions. As shown in Fig. 1, the bearing vibration signal is first inputted into a convolutional layer, followed by BN and ReLU activation function. Its kernel size, stride, and zero padding are 3, 2, and 1, respectively. This convolutional layer transforms the original 1-D signal into a 2-D tensor with 16 channels. Then, a Fourier feature refiner is utilized to refine the features in the frequency domain. Both its amplitude and phase feature refiner are configured to have the same channel number and length as input features. The FFT algorithm utilized in our implementation is provided by PyTorch, supporting parallel computation on GPUs. Next, five soft thresholding-based residual blocks are stacked with the number of channels progressively escalating in powers of 2, i.e., starting from 16 channels and culminating at 512 channels. Within each of these blocks, the convolutional layer is also configured with a kernel size, stride, and zero padding being 3, 2, and 1, respectively. Subsequently, the acquired high-level features are fed into a fully connected layer for final classification. Cross-entropy loss is adopted to measure the distance between the prediction label and the real label. It can be described as follows:

$$\mathcal{L}(y, \widehat{y}) = -\frac{1}{N}\sum_{i=1}^{N} y_i \log(\widehat{y}_i) \tag{18}$$

where y_i represents the label for the ith class, $\widehat{y}_i$ represents the prediction probability for the ith class, and N represents the number of classes.

III. Experimental Validation

A. Experimental Setting

In this article, the proposed framework is implemented by PyTorch with RTX 4090. All data being used in the experiment is Z-score normalized before input into the network to make the training process stable. The optimization algorithm is Adam, with a learning rate of 0.001. The batch size is 128, and the epoch is 100. Each data set used in the experiments will be randomly divided into two parts: 75% is used as a train set, while the remaining 25% is used as a test set. To evaluate the performance of Soft-FFRNet, accuracy and F1-score are adopted. These metrics are derived from four parameters: 1) true positive (TP); 2) true negative (TN); 3) false positive (FP); and 4) false negative (FN). The terms "True" and "False" signify whether the prediction aligns with the true label, while the terms "Positive" and "Negative" signify whether the corresponding class exists according to the prediction. We have

$$\text{Accuracy} = \frac{\text{TP} + \text{TN}}{\text{TP} + \text{TN} + \text{FP} + \text{FN}} \times 100\% \tag{19}$$

$$\text{Precision} = \frac{\text{TP}}{\text{TP} + \text{FP}} \times 100\% \tag{20}$$

$$\text{Recall} = \frac{\text{TP}}{\text{TP} + \text{FN}} \times 100\% \tag{21}$$

$$F1 - \text{score} = 2 \times \frac{\text{precision} \times \text{recall}}{\text{precision} + \text{recall}} \times 100\%. \tag{22}$$

All experiments were repeated four times. Their mean and standard deviation are collected as the final results to enhance the experiment's reliability.

To verify the effectiveness of the proposed Soft-FFRNet, the HSA bearing data set and the motor bearing data set are used. In this section, we conducted an ablation study to validate the effect of the proposed Fourier feature refiner and soft thresholding-based residual block. In addition, the proposed Soft-FFRNet is also compared with other state-of-the-art methods.

The collected signals already inherently include a certain amount of noise. Nevertheless, in practical scenarios, since the real machines are much more complex than the test rig being used to collect data, the signal may contain higher levels of noise. To prove the performance of noise robustness, all experiment will be conducted under several different levels of additional Gaussian white noises, which has a signal-to-noise ratio (SNR) of 0, -2, and -4 dB, respectively. The SNR is calculated as follows:

$$\text{SNR} = 10\log_{10}\left(P_{\text{signal}}/P_{\text{noise}}\right) \tag{23}$$

where P_{signal} and P_{noise} are the power of signal and the noise, respectively.

B. High-Speed Aeronautical Bearing Data Set

1) Data Description: This data set comes from the test rig introduced in [33]. The configuration of the test rig, the test bearing, and the placement of the acceleration sensor can be observed in Fig. 3. The test rig primarily consists of a high-speed spindle responsible for driving the rotation of the shaft. In Fig. 3(b), two triaxial IEPE accelerometers are positioned

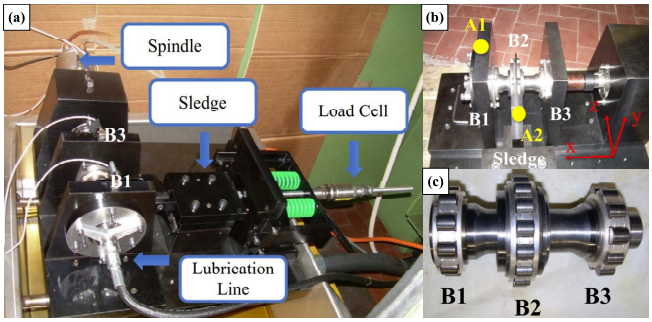

Fig. 3. HSA bearings test rig: (a) general view of the test rig; (b) positions of the accelerometers and the reference system; and (c) shaft with its three roller bearings.

TABLE I
HEALTHY STATE OF HSA DATA SET

Defect	Dimension (μm)
No defect (C1)	-
Diameter of an indentation on the inner ring (C2)	450
Diameter of an indentation on the inner ring (C3)	250
Diameter of an indentation on the inner ring (C4)	150
Diameter of an indentation on a roller (C5)	450
Diameter of an indentation on a roller (C6)	250
Diameter of an indentation on a roller (C7)	150

at A1 and A2, with a sampling frequency of 51 200 Hz. In Fig. 3(c), the inner rings of the bearings (B1, B2, and B3) are connected to a specially designed short and thick hollow shaft, capable of accommodating speeds up to 35 000 rpm.

Table I displays the seven health states assigned to the B1 bearing during signal collection. One state represents a healthy condition (C1), while the remaining six states represent different failure conditions (C2–C7). The identified faults primarily include inner ring faults and roller faults. Each fault type encompasses three different fault sizes, characterized by fault diameters of 150, 250, and 450 μm, respectively. Since the HSA bearing data sets were employed in the experiment, it was conducted under various load and speed conditions. The load is varying from 0 to 1800 N, while the speed is varying from 100 to 500 Hz, where 100 Hz corresponds to 6000 rpm.

To enhance the data, a sliding segmentation method was employed in this experiment. The signal samples were set to a length of 4096×1, resulting in a total of 22 134 training samples and 7259 test samples.

2) Ablation Study: In this section, we conduct an ablation study to demonstrate the effectiveness of each proposed module. The comparison network architectures used are baseline, Soft-Net, FFRNet, and Soft-FFRNet. Baseline: this network architecture merely uses one convolutional layer and five one-layer convolutional residual blocks with an ReLU activation function and a classification layer. Soft-Net: compared with baseline, it replaces the ReLU activation function with a soft-thresholding function, i.e., using the proposed soft thresholding-based residual block. FFRNet: this network architecture adds a Fourier feature refiner after the first convolutional layer. Soft-FFRNet: the proposed framework introduced in Section II. It employs both Fourier feature refiner and soft thresholding-based residual blocks. The experimental results are shown in Table II and visually represented in Fig. 4.

As shown in Table II, when the Gaussian white noise is added, the diagnostic accuracy of baseline plummets, this highlights the poor noise robustness and the inadequacies in frequency domain learning ability of traditional CNN. It is vulnerable to noise, especially under highly noisy conditions like SNR $= -4$ dB, which only has 41.57% diagnostic accuracy. After utilizing the soft-thresholding mechanism, the accuracy of Soft-Net has significantly exceeded baseline by 28.83%, 32.18%, and 32.27%, respectively, under the noise level of SNR $= 0, -2$, and -4 dB. It illustrates the efficiency of the proposed soft thresholding-based residual block in retaining the fault-related information while trimming noise-related information. Similarly, after employing the Fourier feature refiner, the diagnostic accuracy of FFRNet dramatically surpasses the baseline by 35.32%, 43.54%, and 50.29%, respectively, under the noise level of SNR $= 0, -2$, and -4 dB. This reveals that the proposed Fourier feature refiner possesses exceptional frequency domain learning ability, enabling it to extract essential information from highly noisy features.

Nevertheless, under highly noisy conditions, SNR $= -4$ dB, Soft-Net, and FFRNet also deteriorated. This indicates that relying on a single method for denoising is inadequate under high-noise conditions. The proposed Soft-FFRNet reaches 98.83%, 97.48%, and 95.13%, respectively, under the noise level of SNR $= 0, -2$, and -4 dB, showing the extraordinary noise robustness of the proposed framework. It still maintains the diagnostic accuracy of 95.13% when SNR $= -4$ dB, outperforming the Soft-Net and FFRNet by 21.29% and 3.27%, respectively. Meanwhile, in lower noise conditions, SNR $= 0$ and -2 dB, Soft-FFRNet can also exhibit superior performance compared to Soft-Net and FFRNet.

To further illustrate the diagnostic accuracy, Fig. 5 shows the confusion matrixes of baseline, Soft-Net, FFRNet, and Soft-FFRNet when SNR $= -4$ dB. The rows of matrixes denote true labels, and their columns denote predicted labels. The values in the blue cells along the diagonal represent the health states that have been correctly diagnosed. The last column represents the number of test samples for each health state, which is 1037 in this case, revealing a highly balanced distribution of test samples across each health state within the data set. In Fig. 5, it is evident that the proposed Soft-FFRNet outperforms the other three comparative methods in both recall and precision across all health states, demonstrating its consistent improvement in fault diagnosis in highly noisy conditions. Among the seven health states, C4 and C6 are the most challenging to recognize. For both Soft-Net and FFRNet, the recall and precision for these two health states drop to below 90%. However, it is worth noting that our proposed method maintains both recall and precision over 92% for all health states. The metric F1-score shows the same trend as accuracy, underscoring the effectiveness of the proposed method.

In summary, the introduction of a Fourier feature refiner and soft thresholding-based residual block has proven highly

TABLE II
ABLATION STUDY OF THE PROPOSED METHOD ON THE HSA BEARING DATA SET

Noise	Metric	Baseline	Soft-Net	FFRNet	Soft-FFRNet
0dB	Accuracy	62.05±0.71	90.88±0.26	97.37±0.26	**98.83±0.14**
	F1-score	62.18±0.57	90.89±0.26	97.37±0.26	**98.83±0.14**
-2dB	Accuracy	51.88±0.99	84.06±0.67	95.42±0.44	**97.48±0.23**
	F1-score	51.89±1.17	84.09±0.67	95.43±0.44	**97.49±0.23**
-4dB	Accuracy	41.57±1.12	73.84±0.48	91.86±0.81	**95.13±0.55**
	F1-score	41.50±1.20	73.91±0.45	91.87±0.81	**95.13±0.55**

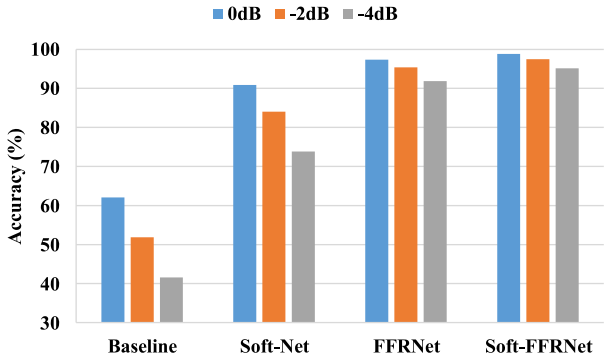

Fig. 4. Accuracy of baseline, Soft-Net, FFRNet, and Soft-FFRNet on the HSA bearing data set.

effective. They noticeably enhance the noise robustness of traditional CNN.

3) Comparing Existing Methods: In this section, the proposed Soft-FFRNet is compared with five existing methods that have good performance in machinery fault diagnosis: 1) MWA-CNN [34]; 2) MA1DCNN [35]; 3) WenCNN [36]; 4) MCSwin-T [37]; and 5) Convformer [38]. MWA-CNN innovatively integrating signal processing theory to enhance interpretability. It alternately employs discrete wavelet attention layer (DWA-layer) and convolutional layer for signal decomposition and feature learning. Furthermore, it introduces a frequency attention mechanism to enhance the ability of MWA-CNN to obtain fault-related features from different frequency components. MA1DCNN introduces two attention modules designed specifically for rolling bearing faults. They are used jointly in MA1DCNN to adaptively recalibrate features of each layer and can enhance the feature learning of fault impulses. WenCNN employs a conversion method that converts signals into 2-D images as input and proposes a new CNN-based fault diagnosis model. MCSwin-T proposed a multichannel calibrated transformer with shifted windows for computing self-attention in each nonoverlapping window, capturing relations between sequences of split patches. Moreover, it utilizes a novel partitioning approaches to establish the connections across windows. Convformer is proposed to extract robust features that integrate both global and local information. It uses sparse modified multiple self-attention to model the long-range dependency of the features while keeping attention on local features. The same training strategy is applied to these methods. The results are shown in Table III and visually represented in Fig. 6.

As shown in Table III, Soft-FFRNet achieves the best performance across all three levels of noise. When SNR $= 0$ dB, the diagnostic accuracy of Soft-FFRNet reaches 98.83%, while the diagnostic accuracies of the other five comparative methods, except for MWA-CNN, drop below 90%. As the level of noise escalates, the diagnostic accuracies of all five comparative methods experience a precipitous decline, plummeting below 90%. However, the proposed Soft-FFRNet stands out once again, maintaining a diagnostic accuracy above 95% even when SNR $= -4$ dB. This indicates a significant gap in noise robustness between the five comparative methods and the proposed method. The ability of Soft-FFRNet to sustain high diagnostic performance under highly noisy conditions demonstrates its efficacy in real-world IIoT systems where ambient noise is a pervasive challenge.

Under highly noisy conditions, the performance of other comparative methods shows a noticeable degradation. However, Soft-FFRNet, leveraging its frequency-domain learning capabilities and adaptive thresholds, showcases remarkable noise robustness.

In summary, thanks to the frequency-domain learning capabilities and adaptive thresholds provided by Soft-FFRNet, the proposed method exhibits excellent noise robustness and can provide excellent diagnostic accuracy under highly noisy conditions. The experiment demonstrates that the Soft-FFRNet is a promising solution for machinery fault diagnosis in IIoT systems.

C. Motor Bearing Data Set

1) Data Description: This data set comes from the experiment platform introduced in [39]. Fig. 7 illustrates the test rig employed in the experiment, along with the fault information and working status of the experimental bearing. The test rig comprises several modules, including an electric motor, a torque measurement shaft, a rolling bearing test module, a flywheel, and a load motor. Experimental bearings with diverse failure modes are installed within the bearing test module to collect the experimental data. It is important to note that the failures observed in the experimental bearings are genuine and not artificially induced. The faults primarily occur in the inner ring and outer ring, with the failure modes being predominantly fatigue pitting and plastic deformations.

As depicted in Table IV, the data set is classified into five distinct fault categories, in addition to the normal category, resulting in a total of six categories. The experiment is carried

Baseline

True Label \ Predicted Label	C1	C2	C3	C4	C5	C6	C7	Recall	Test Number
C1	471	111	141	134	6	67	107	45.42%	1037
C2	182	371	75	104	99	128	78	35.78%	1037
C3	97	72	483	105	14	94	172	46.58%	1037
C4	200	117	103	328	14	104	171	31.63%	1037
C5	45	101	52	61	669	34	75	64.51%	1037
C6	162	202	133	142	59	248	91	23.92%	1037
C7	133	85	164	101	10	49	495	47.73%	1037
Precision	36.51%	35.03%	41.96%	33.64%	76.81%	34.25%	41.63%	-	

Soft-Net

True Label \ Predicted Label	C1	C2	C3	C4	C5	C6	C7	Recall	Test Number
C1	706	47	42	130	4	59	49	68.08%	1037
C2	51	733	16	79	39	57	62	70.68%	1037
C3	15	3	927	4	0	56	32	89.39%	1037
C4	80	63	12	681	4	140	57	65.67%	1037
C5	14	68	0	26	902	16	11	86.98%	1037
C6	52	71	89	107	12	659	47	63.55%	1037
C7	38	74	28	48	10	43	796	76.76%	1037
Precision	73.85%	69.22%	83.21%	63.35%	92.89%	63.98%	75.52%	-	

FFRNet

True Label \ Predicted Label	C1	C2	C3	C4	C5	C6	C7	Recall	Test Number
C1	951	35	15	17	1	8	10	91.71%	1037
C2	11	940	2	30	10	31	13	90.65%	1037
C3	1	2	1005	0	0	26	3	96.91%	1037
C4	14	46	2	907	2	57	9	87.46%	1037
C5	7	6	11	15	989	5	4	95.37%	1037
C6	9	22	24	37	6	932	7	89.87%	1037
C7	6	8	6	12	5	25	975	94.02%	1037
Precision	95.20%	88.76%	94.37%	89.10%	97.63%	85.98%	95.49%	-	

Soft-FFRNet

True Label \ Predicted Label	C1	C2	C3	C4	C5	C6	C7	Recall	Test Number
C1	1011	6	2	7	0	4	7	97.49%	1037
C2	6	998	0	18	3	3	9	96.24%	1037
C3	1	0	1006	2	1	25	2	97.01%	1037
C4	11	29	1	962	0	27	7	92.77%	1037
C5	5	4	0	16	1002	7	3	96.62%	1037
C6	4	12	13	31	1	972	4	93.73%	1037
C7	3	7	3	7	1	10	1006	97.01%	1037
Precision	97.12%	94.51%	98.15%	92.23%	99.40%	92.75%	96.92%	-	

Fig. 5. Confusion matrix of baseline, Soft-Net, FFRNet, and Soft-FFRNet (SNR = −4 dB).

TABLE III
COMPARISON RESULT OF SOFT-FFRNET AND FIVE EXISTING METHODS ON THE HSA BEARING DATA SET

Noise	Metric	Soft-FFRNet	MWA-CNN	MA1DCNN	WenCNN	MCSwin-T	Convformer
0dB	Accuracy	**98.83±0.14**	93.98±0.59	89.08±1.21	86.15±1.18	84.15±0.75	87.35±0.76
	F1-score	**98.83±0.14**	93.98±0.59	89.13±1.20	86.14±1.16	84.17±0.77	87.33±0.75
-2dB	Accuracy	**97.48±0.23**	89.82±1.33	81.29±1.68	76.32±2.50	75.06±1.14	82.06±1.05
	F1-score	**97.49±0.23**	89.84±1.36	81.22±1.85	76.34±2.43	75.08±1.15	82.10±1.11
-4dB	Accuracy	**95.13±0.55**	84.03±0.94	75.08±1.79	63.99±2.24	60.59±1.19	72.74±0.57
	F1-score	**95.13±0.55**	83.96±1.10	75.23±1.76	64.00±2.22	60.49±1.11	72.77±0.56

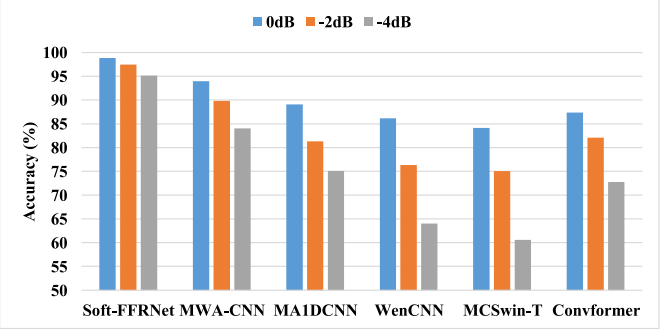

Fig. 6. Accuracy of Soft-FFRNet and five comparison methods on the HSA bearing data set.

out under different conditions. The radial force applied on the bearing is 400 or 1000 N, the load torch is 0.1 or 0.7 Nm, and the rotational speed is 900 or 1500 rpm. Only vibration signal data is used in this experiment, with a sampling frequency of 64 kHz. To augment the signal samples, the sliding segmentation method is applied, and each sample has a length of 5120 × 1. A total of 36 053 training samples and 12 017 test samples were generated as a result.

2) Comparison Study: In this section, the proposed Soft-FFRNet continues to be compared with five existing methods mentioned in the experiment on the HSA bearing data set. The results are shown in Table V and visually represented in Fig. 8.

As shown in Table V, it is evident that the motor bearing data set is not as challenging as the HSA bearing data set under highly noisy conditions. All methods exhibit superior performance compared to their counterparts on the HSA bearing data set.

Notably, the proposed Soft-FFRNet still obtains the best performance across all three levels of noise. When SNR = 0 dB, Soft-FFRNet has a diagnostic accuracy of 99.96%. Particularly, under more adverse conditions, such as when SNR = −4 dB, Soft-FFRNet still maintains a remarkable diagnostic accuracy of 99.15%. In contrast, for most of the comparison methods, their performances experience a noticeable degradation in performance as the noise level increases. For example, when SNR = −4 dB, MCSwin-T exhibits an accuracy of only 90.47% and an F1-score of 90.48%. Similarly, Convformer only has an accuracy of 87.45% and an F1-score of 84.46%. This stark decline in performance underscores the challenges faced by existing methods in maintaining diagnostic accuracy under highly noisy conditions.

The results of this experiment reaffirm the general robustness improvement provided by Soft-FFRNet. The consistently superior performance of Soft-FFRNet across all three levels of

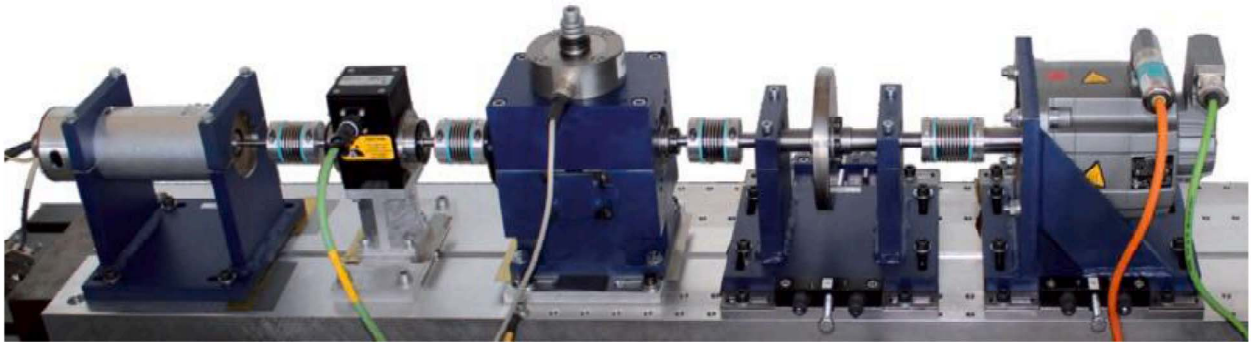

Fig. 7. Motor bearing test rig.

TABLE IV
HEALTHY STATE OF THE MOTOR BEARING DATA SET

Damage	Bearing Element
Normal	-
Fatigue: Pitting	Outer Ring
Plastic Deform.: Indentations	Outer Ring
Fatigue: Pitting	Outer Ring; Inner Ring
Plastic Deform.: Indentations	Outer Ring; Inner Ring
Fatigue: Pitting	Inner Ring

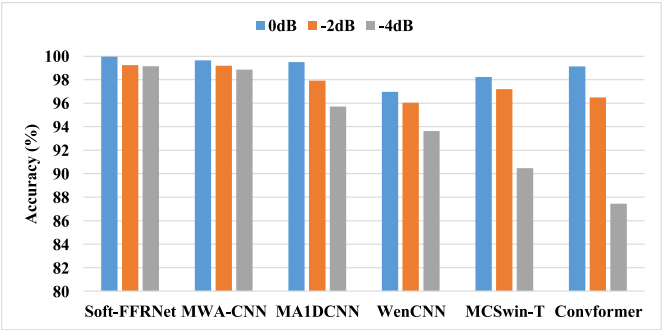

Fig. 8. Accuracy of Soft-FFRNet and five comparison methods on the motor bearing data set.

noise indicates it is a promising and reliable PHM framework for machinery fault diagnosis in IIoT systems.

IV. DISCUSSION

A. Discussion of Practical Applications in IIoT

The proposed Soft-FFRNet, with its emphasis on frequency domain analysis and adaptive noise reduction, holds significant potential for industrial applications within the realm of IIoT. In scenarios where IIoT technologies are employed for machinery fault diagnosis, machines operate in varied conditions. IIoT sensors used to detect the machines may encounter diverse noise environments, in this situation, the proposed method can effectively diagnose the health states machines, facilitating prompt alerts for potential failures. The diagnostic results play a crucial role in decision-making processes for predictive maintenance, replacement, and asset management.

Traditionally, engineers heavily relied on their expert knowledge for fault diagnosis. However, with the rapid development of modern industries, the demand for automatic diagnostic methods has surged. The evolution of IIoT technologies has significantly increased the amount of data available, propelling the development of deep learning-based methods. These methods have gained considerable attention due to their ability to automatically extract rich abstract features from substantial data sets without the need for extensive expert knowledge. However, existing deep learning models face challenges in extracting weak fault-related features from the signals contaminated by strong environmental noise. Therefore, Soft-FFRNet is proposed to address these challenges for the application of machinery fault diagnosis for data acquired from IIoT sensors. This innovative method can promptly and accurately diagnose the health state of machines, preventing the escalation of potential damages and minimizing the likelihood of severe failures.

B. Discussion of Fourier Feature Refiner

Traditionally, machinery fault diagnosis algorithms typically rely on time-domain feature extraction. However, the effectiveness of these methods tends to diminish significantly under highly noisy conditions, since, in the time domain, fault-related features are subtle and are susceptible to being obscured by ambient noise. This inherent limitation underscores the need for innovative approaches that can adapt to challenging noise environments and extract fault-related information more reliably.

The proposed Fourier feature refiner represents a significant departure from the conventional reliance on time-domain features. Leveraging the power of frequency domain learning, this novel module of the diagnostic algorithm capitalizes on the fact that fault-related features are often more pronounced and distinguishable in the frequency domain. This shift in focus allows the algorithm to overcome the challenges posed by noisy conditions and extract fault-related information with enhanced precision.

Each fault type has its unique fault-related frequencies. The integration of frequency domain learning capabilities in the proposed Fourier feature refiner plays an important role in disentangling fault-related frequency components from those influenced by noise. This sophisticated mechanism enables it to discern and emphasize fault-related features, contributing to its robust performance in the presence of strong ambient

TABLE V
COMPARISON RESULT OF SOFT-FFRNET AND FIVE EXISTING METHODS ON THE MOTOR BEARING DATA SET

Noise	Metric	Soft-FFRNet	MWA-CNN	MA1DCNN	WenCNN	MCSwin-T	Convformer
0dB	Accuracy	**99.96±0.01**	99.65±0.14	99.49±0.09	96.97±0.44	98.23±1.56	99.14±0.24
	F1-score	**99.96±0.01**	99.62±0.17	99.44±0.13	97.10±0.37	98.33±1.51	99.10±0.25
-2dB	Accuracy	**99.24±0.21**	99.18±0.14	97.92±0.98	96.03±0.34	97.20±0.87	96.49±1.37
	F1-score	**99.20±0.20**	99.06±0.15	97.56±1.28	96.25±0.34	97.15±0.87	96.08±1.72
-4dB	Accuracy	**99.15±0.29**	98.86±0.20	95.70±2.83	93.63±0.73	90.47±1.61	87.45±3.17
	F1-score	**99.18±0.29**	98.79±0.21	95.39±2.89	93.79±0.49	90.87±1.62	84.46±5.63

noise. The findings highlight its ability to enhance fault-related feature extraction by leveraging the inherent characteristic of frequency domain information.

The experiment section provides empirical evidence of the effectiveness of this approach, showcasing how the Fourier feature refiner successfully disentangles fault-related frequencies from noise-related frequencies under highly noisy conditions.

In summary, the Fourier feature refiner represents a significant advancement in machinery fault diagnosis algorithms, transcending the limitations of traditional time domain-based approaches. By embracing the frequency domain, it becomes a more nuanced and effective method for extracting fault-related features, offering a promising avenue for enhancing the accuracy and reliability of machinery fault diagnosis, especially in environments where ambient noise poses a substantial obstacle.

C. Discussion of Soft Thresholding-Based Residual Block

The variability of noises across diverse working conditions of IIoT sensors underscores the inadequacy of traditional denoising techniques governed by fixed parameters. Recognizing the need for a more adaptive approach, the proposed soft thresholding-based residual block emerges as an effective method to endow the network with adaptive nonlinear thresholds. This novel mechanism goes beyond the constraints of conventional denoising techniques by providing a more sophisticated and adaptive strategy for preserving crucial fault-related features while effectively mitigating the impact of various noises.

The core of the soft thresholding-based residual block lies in its ability to deliver dynamic nonlinear transformations, a critical aspect for extracting meaningful fault-related information amidst changing noise landscapes. The adaptive nature of the soft-thresholding mechanism ensures it can dynamically adjust its response to different types of signals and varying noise conditions. This adaptability proves essential for maintaining the robustness of the proposed network, enabling it to perform consistently under a variety of real-world IIoT sensor operating conditions.

The dynamic threshold adjustment capability of the soft-thresholding mechanism is particularly noteworthy. This feature allows the soft thresholding-based residual block to effectively handle varying noise levels under different working conditions. By dynamically adapting its threshold, the mechanism can distinguish and retain essential fault-related features while diminishing the impact of varying noise components.

Furthermore, the selective elimination of smaller components by the soft-thresholding mechanism contributes to a sparser and more concise representation of fault-related features. This simplified representation facilitates to extraction of the main fault-related components.

The experiment section also provides empirical evidence of the soft thresholding-based residual block's effectiveness in handling various noise levels and preserving fault-related features across diverse working conditions.

In summary, the proposed soft thresholding-based residual block represents a significant advancement in noise reduction and fault-related feature preservation, offering an adaptive and sophisticated solution for machinery fault diagnosis across diverse working conditions of IIoT sensors.

V. CONCLUSION

PHM technologies are crucial not only for saving time and money but also for protecting people's lives. To provide accurate and prompt machinery fault diagnosis for machines in IIoT systems under highly noisy conditions, this article proposes a Soft-FFRNet. Soft-FFRNet is mainly composed of an innovative Fourier feature refiner and multiple soft thresholding-based residual blocks. Based on this, we explore the frequency domain learning mechanism in deep-learning and adaptive noise reduction. The proposed Fourier feature refiner endows the model with frequency domain learning ability, which allows the separation of fault-related frequency components and noise-related frequency components. In addition, the proposed soft thresholding-based residual blocks provide adaptive nonlinear thresholds to tackle various noises under different working conditions, thereby preserving the main fault-related features while reducing noise.

In this article, experiments are performed on the HAS bearing and the motor bearing data sets under three different levels of additional Gaussian white noises. Experimental results show that the proposed Soft-FFRNet can significantly improve diagnostic performance and noise robustness. Also, Soft-FFRNet has better performance than other existing deep learning methods, especially under highly noisy conditions.

The conclusion can be summarized as follows.

1) The Soft-FFRNet is capable of providing accurate and prompt machinery fault diagnosis for machines in IIoT systems under highly noisy conditions.
2) The frequency domain learning is useful to improve the noise robustness of the framework.
3) The soft-thresholding mechanism is beneficial to noise reduction.
4) The Soft-FFRNet has good performance and noise robustness on both data sets. It can effectively diagnose the health states of machines under highly noisy conditions.

To broaden the applicability of our method, future efforts will concentrate on integrating our method with unsupervised domain adaptation techniques. In this manner, the model can transfer the knowledge learned from labeled data sets to unlabeled data sets, which is more commonly encountered in real-life industrial applications due to the high cost of labeling fault types. Moreover, in the future work, we will explore the impact of frequency resolution on the Fourier feature refiner.

REFERENCES

[1] M. Cerrada et al., "A review on data-driven fault severity assessment in rolling bearings," *Mech. Syst. Signal Process.*, vol. 99, pp. 169–196, Jan. 2018.

[2] Y. Lei, B. Yang, X. Jiang, F. Jia, N. Li, and A. K. Nandi, "Applications of machine learning to machine fault diagnosis: A review and roadmap," *Mech. Syst. Signal Process.*, vol. 138, Apr. 2020, Art. no. 106587.

[3] Y. Feng, J. Chen, Z. Liu, H. Lv, and J. Wang, "Full graph autoencoder for one-class group anomaly detection of IIoT system," *IEEE Internet Things J.*, vol. 9, no. 21, pp. 21886–21898, Nov. 2022.

[4] X. Wang et al., "Toward accurate anomaly detection in Industrial Internet of Things using hierarchical federated learning," *IEEE Internet Things J.*, vol. 9, no. 10, pp. 7110–7119, May 2022.

[5] Y. Song, S. Gao, Y. Li, L. Jia, Q. Li, and F. Pang, "Distributed attention-based temporal convolutional network for remaining useful life prediction," *IEEE Internet Things J.*, vol. 8, no. 12, pp. 9594–9602, Jun. 2021.

[6] M. Compare, P. Baraldi, and E. Zio, "Challenges to IoT-enabled predictive maintenance for industry 4.0," *IEEE Internet Things J.*, vol. 7, no. 5, pp. 4585–4597, May 2020.

[7] L. Ren, Y. Liu, X. Wang, J. Lü, and M. J. Deen, "Cloud—Edge-based lightweight temporal convolutional networks for remaining useful life prediction in IIoT," *IEEE Internet Things J.*, vol. 8, no. 16, pp. 12578–12587, Aug. 2021.

[8] D. Peng, Z. Liu, H. Wang, Y. Qin, and L. Jia, "A novel deeper one-dimensional CNN with residual learning for fault diagnosis of wheelset bearings in high-speed trains," *IEEE Access*, vol. 7, pp. 10278–10293, 2019.

[9] J. Sun, C. Yan, and J. Wen, "Intelligent bearing fault diagnosis method combining compressed data acquisition and deep learning," *IEEE Trans. Instrum. Meas.*, vol. 67, no. 1, pp. 185–195, Jan. 2018.

[10] Y. Lei, *Intelligent Fault Diagnosis and Remaining Useful Life Prediction of Rotating Machinery*. Oxford, U.K.: Butterworth-Heinemann, 2016.

[11] A. N. Tikhonov and V. Arsenin, *Solutions of Ill-Posed Problems*. New York, NY, USA: Wiley, 1977.

[12] D. E. Rumelhart, G. E. Hinton, and R. J. Williams, "Learning representations by back-propagating errors," *Nature*, vol. 323, no. 6088, pp. 533–536, 1986.

[13] Y. Yu and C. Junsheng, "A roller bearing fault diagnosis method based on EMD energy entropy and ANN," *J. Sound Vibrat.*, vol. 294, nos. 1–2, pp. 269–277, 2006.

[14] C. Cortes and V. Vapnik, "Support-vector networks," *Mach. Learn.*, vol. 20, pp. 273–297, Sep. 1995.

[15] M. Unal, M. Onat, M. Demetgul, and H. Kucuk, "Fault diagnosis of rolling bearings using a genetic algorithm optimized neural network," *Measurement*, vol. 58, pp. 187–196, Dec. 2014.

[16] J. Zheng, H. Pan, and J. Cheng, "Rolling bearing fault detection and diagnosis based on composite multiscale fuzzy entropy and ensemble support vector machines," *Mech. Syst. Signal Process.*, vol. 85, pp. 746–759, Feb. 2017.

[17] H. Liu, J. Zhou, Y. Zheng, W. Jiang, and Y. Zhang, "Fault diagnosis of rolling bearings with recurrent neural network-based autoencoders," *ISA Trans.*, vol. 77, pp. 167–178, Jun. 2018.

[18] F. Zhou, S. Yang, H. Fujita, D. Chen, and C. Wen, "Deep learning fault diagnosis method based on global optimization GAN for unbalanced data," *Knowl. Based Syst.*, vol. 187, Jan. 2020, Art. no. 104837.

[19] T. De Bruin, K. Verbert, and R. Babuška, "Railway track circuit fault diagnosis using recurrent neural networks," *IEEE Trans. Neural Netw. Learn. Syst.*, vol. 28, no. 3, pp. 523–533, 2016.

[20] W. Li, Z. Shang, M. Gao, S. Qian, B. Zhang, and J. Zhang, "A novel deep autoencoder and hyperparametric adaptive learning for imbalance intelligent fault diagnosis of rotating machinery," *Eng. Appl. Artif. Intell.*, vol. 102, Jun. 2021, Art. no. 104279.

[21] X. Zhang, X. Zhang, J. Liu, B. Wu, and Y. Hu, "Graph features dynamic fusion learning driven by multi-head attention for large rotating machinery fault diagnosis with multi-sensor data," *Eng. Appl. Artif. Intell.*, vol. 125, Oct. 2023, Art. no. 106601.

[22] T. Jin, C. Yan, C. Chen, Z. Yang, H. Tian, and S. Wang, "Light neural network with fewer parameters based on CNN for fault diagnosis of rotating machinery," *Measurement*, vol. 181, Aug. 2021, Art. no. 109639.

[23] X. Li, H. Jiang, R. Wang, and M. Niu, "Rolling bearing fault diagnosis using optimal ensemble deep transfer network," *Knowl. Based Syst.*, vol. 213, Feb. 2021, Art. no. 106695.

[24] X. Jiang, X. Li, Q. Wang, Q. Song, J. Liu, and Z. Zhu, "Multi-sensor data fusion-enabled semi-supervised optimal temperature-guided PCL framework for machinery fault diagnosis," *Inf. Fus.*, vol. 101, Jan. 2024, Art. no. 102005.

[25] C. Yang, Z. Qiao, R. Zhu, X. Xu, Z. Lai, and S. Zhou, "An intelligent fault diagnosis method enhanced by noise injection for machinery," *IEEE Trans. Instrum. Meas.*, vol. 72, pp. 1–11, Oct. 2023.

[26] B. Zhao, X. Zhang, H. Li, and Z. Yang, "Intelligent fault diagnosis of rolling bearings based on normalized CNN considering data imbalance and variable working conditions," *Knowl. Based Syst.*, vol. 199, Jul. 2020, Art. no. 105971.

[27] Y. Xu et al., "Multiattention-based feature aggregation convolutional networks with dual focal loss for fault diagnosis of rotating machinery under data imbalance conditions," *IEEE Trans. Instrum. Meas.*, vol. 73, pp. 1–11, Jan. 2024.

[28] J. Wang, R. Ran, and B. Fang, "GNPENet: A novel convolutional neural network with local structure for fault diagnosis," *IEEE Trans. Instrum. Meas.*, vol. 73, pp. 1–16, 2024.

[29] X. Lin, B. Li, X. Yang, and J. Wang, "Fault Diagnosis of aero-engine bearing using a stacked auto-encoder network," in *Proc. IEEE 4th Inf. Technol. Mechatron. Eng. Conf. (ITOEC)*, 2018, pp. 545–548.

[30] Y. Huang, Z. Xu, T. Shan, L. Cao, J. Wang, and Y. Shen, "Fault diagnosis of aviation bearing based on enhanced multi fractional domain feature," in *Proc. IEEE Int. Conf. Sens., Diagn., Progn., Control (SDPC)*, 2022, pp. 57–61.

[31] D. L. Donoho, "De-noising by soft-thresholding," *IEEE Trans. Inf. Theory*, vol. 41, no. 3, pp. 613–627, May 1995.

[32] M. Zhao, S. Zhong, X. Fu, B. Tang, and M. Pecht, "Deep residual shrinkage networks for fault diagnosis," *IEEE Trans. Ind. Informat.*, vol. 16, no. 7, pp. 4681–4690, Jul. 2020.

[33] A. P. Daga, A. Fasana, S. Marchesiello, and L. Garibaldi, "The Politecnico di Torino rolling bearing test rig: Description and analysis of open access data," *Mech. Syst. Signal Process.*, vol. 120, pp. 252–273, Apr. 2019.

[34] H. Wang, Z. Liu, D. Peng, and M. J. Zuo, "Interpretable convolutional neural network with multilayer wavelet for noise-robust machinery fault diagnosis," *Mech. Syst. Signal Process.*, vol. 195, Jul. 2023, Art. no. 110314.

[35] H. Wang, Z. Liu, D. Peng, and Y. Qin, "Understanding and learning discriminant features based on multiattention 1DCNN for wheelset bearing fault diagnosis," *IEEE Trans. Ind. Informat.*, vol. 16, no. 9, pp. 5735–5745, Sep. 2020.

[36] L. Wen, X. Li, L. Gao, and Y. Zhang, "A New convolutional neural network-based data-driven fault diagnosis method," *IEEE Trans. Ind. Electron.*, vol. 65, no. 7, pp. 5990–5998, Jul. 2018.

[37] Z. Chen, J. Chen, S. Liu, Y. Feng, S. He, and E. Xu, "Multi-channel calibrated transformer with shifted windows for few-shot fault diagnosis under sharp speed variation," *ISA Trans.*, vol. 131, pp. 501–515, Dec. 2022.

[38] S. Han, H. Shao, J. Cheng, X. Yang, and B. Cai, "Convformer-NSE: A novel end-to-end gearbox fault diagnosis framework under heavy noise using joint global and local information," *IEEE/ASME Trans. Mechatron.*, vol. 28, no. 1, pp. 340–349, Feb. 2023.

[39] C. Lessmeier, J. K. Kimotho, D. Zimmer, and W. Sextro, "Condition monitoring of bearing damage in electromechanical drive systems by using motor current signals of electric motors: A benchmark data set for data-driven classification," in *Proc. PHM Soc. Eur. Conf.*, vol. 3, 2016, pp. 1–17.

Huan Wang (Graduate Student Member, IEEE) born in Hunan, China, in 1994. He received the B.S. and M.S. degrees in mechanical engineering from the University of Electronic Science and Technology of China, Chengdu, China, in 2016 and 2021, respectively. He is currently pursuing the Ph.D. degree in management science and engineering with Tsinghua University, Beijing, China.

He has authored or coauthored over 40 articles, including more than 20 journal articles indexed by the Science Citation Index and three Essential Science Indicators highly cited articles. His research interests include prognostics and health management for electromechanical systems, remaining useful life estimation, deep learning, and machine learning.

Mr. Wang has won two best conference paper awards and five international data challenge awards. He is also a peer-reviewed reviewer for more than ten international journals.

Wenjun Luo was born in Jiangsu, China, in 2001. He is currently pursuing the B.S. degree in electronic and electrical engineering with the University of Electronic Science and Technology of China, Chengdu, China.

His research interests include deep learning, attention mechanism, computer vision, defect recognition, prognostics and health management, and fault diagnosis.

Zhiliang Liu (Member, IEEE) was born in Rizhao, Shandong, China, in 1984. He received the Ph.D. degree from the School of Automation Engineering, University of Electronic Science and Technology of China (UESTC), Chengdu, China, in 2013.

From 2009 to 2011, he studied with the University of Alberta, Edmonton, AB, Canada, as a Visiting Scholar. From 2013 to 2015, he was an Assistant Professor with the UESTC's School of Mechanical and Electrical Engineering, where he has been an Associate Professor since 2015. He currently holds more than 20 research grants from the National Natural Science Foundation of China, Open Grants of National Key Laboratory, and China Postdoctoral Science Foundation. He has published more than 120 papers, including more than 50 SCI-Indexed journal papers. His research interests include fault diagnosis and prognostics of rotating machinery by using advanced signal processing and data-mining methods.

Junhao Zhang (Graduate Student Member, IEEE) was born in Sichuan, China, in 1999. He received the B.S. degree in communication engineering from the University of Electronic Science and Technology of China, Chengdu, China, in 2021. He is currently pursuing the Ph.D. degree in electrical and electronic engineering with Nanyang Technological University, Singapore.

His research interests include deep learning, machine learning, computer vision, and fault diagnosis.

Mingjian Zuo (Senior Member, IEEE) received the B.Sc. degree in agricultural engineering from the Shandong Institute of Technology, Zibo, China, in 1982, and the M.Sc. and Ph.D. degrees in industrial engineering from Iowa State University, Ames, IA, USA, in 1986 and 1989, respectively.

He is a Principal Scientist with Qingdao International Academician Park Research Institute, Qingdao, China, a Guest Professor with the University of Electronic Science and Technology of China, Chengdu, China, and a Full Professor with the University of Alberta, Edmonton, AB, Canada. His research interests include system reliability analysis, maintenance modeling and optimization, signal processing, and fault diagnosis.

Dr. Zuo served as a Department Editor for Institute of Industrial and Systems Engineers (IISE) Transactions, an Associate Editor for IEEE TRANSACTIONS ON RELIABILITY, *Journal of Risk and Reliability*, and *International Journal of Reliability, Quality and Safety Engineering*, a Regional Editor for *International Journal of Strategic Engineering Asset Management*, and an Editorial Board Member for *Reliability Engineering and System Safety*, *Journal of Traffic and Transportation Engineering*, and *International Journal of Performability Engineering*. He is a Fellow of the Canadian Academy of Engineering, IISE, and the Engineering Institute of Canada, and a Founding Fellow of the International Society of Engineering Asset Management.